Lumping of the low temperature oxidation of n-pentane: application of MEL

L. Pratali Maffei[1], M. Pelucchi[*, 1], T. Faravelli[1]

[1] CRECK Modeling Lab – Department of Chemistry, Materials and Chemical Engineering, Politecnico di Milano, 20133 Milano, Italy

Abstract

We recently developed a lumping code (MEL) that allows to lump automatically the reactivity of one potential energy surface (PES) to reduce the overall number of species and reactions and facilitate its integration in global combustion kinetic schemes. In this work, we extend the application of MEL to the lumping of multiple PESs in existing detailed kinetic schemes. In particular, the low temperature oxidation kinetic subset of n-pentane by Bugler et al. is reduced from 81 species and 151 reactions to 20 species and 56 reactions. The lumping procedure is completely independent of simulations of ideal reactors experiments. The performance of the lumped mechanism is almost identical to the original kinetic scheme in the simulated jet stirred reactor, shock tube and rapid compression machine experiments, showing the potential and the accuracy of the approach proposed.

Introduction

The intrinsically large size of detailed chemical kinetic mechanisms for the combustion of hydrocarbon species has motivated the development of several chemical lumping and reduction procedures [1]. In fact, chemical reduction is essential for both the fundamental understanding of the combustion chemistry, avoiding overcomplicated pathways not necessarily deserving a detailed description, and the use of kinetic mechanisms in computational fluid dynamics simulations. In the past decades, the large number of theoretical studies to determine more accurate rate constants and to discover new reaction pathways further increased the already large size of detailed kinetic mechanisms, resulting in kinetic schemes of hundreds of species and thousands of reactions, even for relatively small fuels. In particular, the use of ab initio transition state theory-based master equation (AITSTME) methodologies for the exploration of complex potential energy surfaces (PESs) has become increasingly popular thanks to the availability of both higher computational power and automatic routines for theoretical calculations. However, the update of existing kinetic schemes with the rate constants of complex multi-well PESs such as those describing the low temperature pathways for alkene oxidation (e.g. $R+O_2$, [2]) or aromatic hydrocarbons oxidation pathways (e.g. C_5H_5+OH, [3]) is still a challenging theoretical task. One of the main problems relates to the inclusion of a large number of additional species, mostly not showing any significant secondary reactivity nor accumulating at any operating conditions of interest. This complicates the reaction network as well as the understanding of the occurring chemical phenomena.

To address these issues, we recently developed a master equation lumping approach (MEL) automatically implemented with a Python code available on GitHub (https://github.com/lpratalimaffei/MEL) [4]. MEL is designed to process the output of master equation calculations of a multi-well PES, or, in fact, any detailed kinetic mechanism describing the reactivity of multiple interconnected isomers on one PES. In particular, MEL allows to merge together species with similar chemical behavior and to treat implicitly the reactivity of unstable isomers. The overall reactivity of the detailed mechanism is thus reproduced with a smaller set of equivalent rate constants which retain the chemical meaning of the original mechanism. MEL treats single PESs similarly to traditional "horizontal" lumping approaches [5], however it does not require any experimental data or experience-based assumptions. Furthermore, although the approach provides indications about appropriate constituents of pseudospecies and unstable redundant species, the user is still free to impose constraints on the selected species and on the extent of the lumping (e.g. products of a given reaction may retain the original level of detail). Finally, our approach provides the composition of each pseudospecies as a function of temperature and pressure. Hence, the secondary reactivity of one specific isomer may still be introduced in the kinetic scheme by weighing it properly according to the fraction of the selected isomer in its pseudospecies (i.e. *delumping* procedure). We proved the accuracy and the potential of MEL by applying it successfully to several PESs for relevant reaction classes in monoaromatic hydrocarbons pyrolysis and oxidation [4,6,7].

In this work, we extend the application of MEL to the low-temperature oxidation chemistry of n-pentane, considered large enough to be representative of larger alkanes yet small enough for a detailed and complete study of low-temperature oxidation pathways. The renewed interest in the low-temperature chemistry of n-alkanes oxidation [8–11] is related to both their importance in practical combustion applications and to the advancement of new engine technologies (e.g. gasoline compression-ignition engines). This motivated theoretical investigations of new reaction pathways and the revision of detailed kinetic models according to new reaction classes and rate rules. In particular, Bugler et al. recently revised the detailed modeling of the low temperature oxidation of n-pentane, highlighting the

* Corresponding author: matteo.pelucchi@polimi.it

relevance of accurate thermochemistry, appropriate updated rate rules for the main reaction classes, and the impact of the newly introduced reactivity of hydroperoxyl-alkyl-peroxyl radicals [9]. This model was further updated and validated against data from shock tube, rapid compression machine and jet stirred reactor experiments [12,13]. The description of n-pentane oxidation chemistry is extremely detailed and rigorous and includes a large number of isomers, making it suitable for the application of our automatic lumping procedure.

n-pentane low temperature oxidation kinetics

Figure 1 summarizes the kinetic scheme of the primary oxidation reactions of n-pentyl radicals of the mechanism of Bugler et al. [12]. Molecular oxygen addition to three different n-pentyl radicals forms three RO_2 isomers which either eliminate HO_2 or isomerize to hydroperoxyl-alkyl (QOOH) radicals. QOOH radicals may form olefins+HO_2, cyclic ethers+OH, or decompose to various beta-scission products. A second O_2 addition to QOOH radicals to form hydroperoxyl-alkyl-peroxyl radicals O_2QOOH leads to analogous pathways involving dihydroperoxyl-alkyl radicals $P(OOH)_2$. Contrary to RO_2 radicals, O_2QOOH radicals produce an important fraction of carbonyl-hydroperoxides+OH. As highlighted by Bugler et al. [12], the inclusion of the reactivity of $P(OOH)_2$ radicals into n-pentane oxidation mechanism is essential to reproduce its low temperature combustion behavior. However, these reaction pathways involve a large number of isomers often taking part to very few reactions (in some cases, one or two). Similarly, $P(OOH)_2$ decomposition products consist of several isomers further dissociating to smaller species. Therefore, reducing the number of species and reactions describing n-pentane low-temperature oxidation pathways would both simplify the understanding of their role in the global reaction network and decrease the computational time of reactor simulations.

This work addresses the lumping of RO_2 and RO_4 PESs accessed from the O_2 additions to the various fuel radicals and hydroperodyl-alkyl radicals. The two main challenges consist in grouping together the isomers into appropriate pseudospecies and describing accurately their secondary reactivity. In fact, lumping the products of these PESs such as cyclic ethers or carbonyl-hydroperoxides also implies the lumping of all their successive decomposition reactions. First, we lumped the RO_2 PES; the information about the QOOH radicals distribution was then used to lump the RO_4 PES. Finally, the secondary reactivity of the products of both PESs was also lumped. The procedure is reporter in greater detail in the following sections.

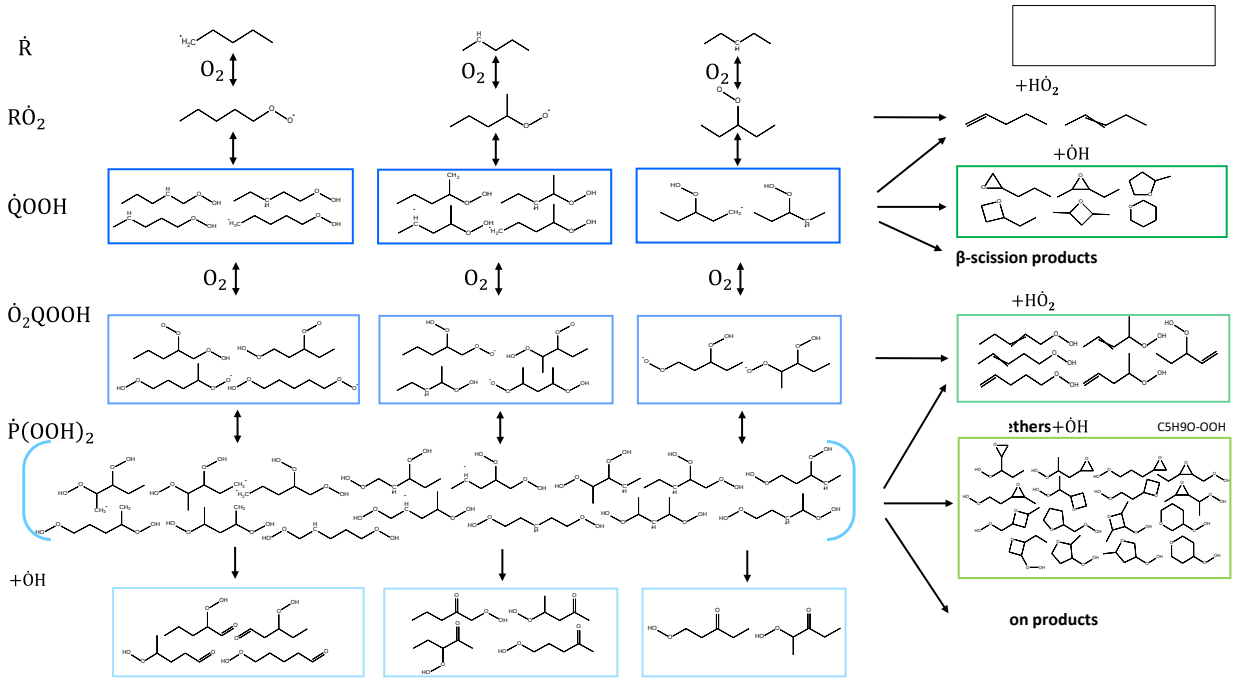

Figure 1: Schematic representation of the detailed kinetics of the low-temperature oxidation of n-pentane in the mechanism of Bugler et al. [12]. All isomers of the original kinetic mechanism are shown. Colored boxes group together the isomers merged as one pseudospecies in the lumped mechanism. Brackets indicate isomers removed in the final lumped mechanism. Species names are those used in the final lumped mechanism.

Lumping of R+O_2 and QOOH+O_2 PESs

The lumped species and products of RO_2 and RO_4 PESs are schematically represented in Figure 1, where merged groups of species are enclosed in boxes. The scheme highlights the extent of species reduction: only 20 pseudospecies were obtained from an initial set of 81 species.

RO_2 PES is accessed via molecular oxygen addition to three different pentyl isomers, i.e. C_5H_{11}-1, C_5H_{11}-2, C_5H_{11}-3, forming $C_5H_{11}O_2$-1, $C_5H_{11}O_2$-2, $C_5H_{11}O_2$-3. The

species names used in this section correspond to those of the detailed and lumped mechanisms. Each alkyl-peroxyl radical isomerizes to various hydroperoxyl-alkyl-peroxyl-radicals QOOH. Although the beta-scission products are different, the three RO_2 radicals eventually form the same pool of olefins and cyclic ethers, which share similar secondary reactivity. Thus, we decided to keep the three RO_2 radicals and we lumped the QOOH isomers formed by each of them in three groups, whereas all the cyclic ethers were merged together as one pseudospecies. The reasons for this choice are related to the structure of the detailed mechanism: lumping together all RO_2 isomers requires the knowledge of the composition of the n-pentyl radical pool. Although at low temperatures it depends mostly on the rate constants of H-atom abstraction reactions, we found that the temperature-dependent branching fractions (BFs) of C_5H_{11}-1,2,3 vary with the abstracting radical. Furthermore, at higher temperatures also n-pentane bond-fission and isomerization reactions among pentyl radicals play a role. Because these reactions are pressure-dependent in the detailed mechanism, deriving a proper composition for n-pentyl valid at all conditions would also imply introducing pressure dependence in most n-pentyl secondary reactions.

The lumping of the reactivity of each n-pentyl+O_2 sub-PES was done according to the procedure described in detail in our recent work [4] and briefly recalled here. First, the set of $\tilde{N}$ pseudospecies including unmerged (e.g. C_5H_{11}-1, $C_5H_{11}O_2$-1, see Figure 1) and merged (e.g. $C_5H_{10}OOH$-1, $C_5H_{10}O$) species is defined. Then, lumped rate constants are derived for each pseudospecies. This requires to solve the problem of reducing the ODE system describing the initial set of N species $\frac{d\mathbf{c}}{dt} = \mathbf{Kc}$ (where $\mathbf{K}$ is the matrix of rate constants of the detailed mechanism and $\mathbf{c}$ is the species concentration) to the equivalent lumped system for $\tilde{N} < N$ pseudospecies $\frac{d\tilde{\mathbf{c}}}{dt} = \tilde{\mathbf{K}}\tilde{\mathbf{c}}$. The system $\frac{d\mathbf{c}}{dt} = \mathbf{Kc}$ describing the evolution of the N species is solved in $\tilde{N}$ sets of simulations: in each set, one of the $\tilde{N}$ pseudospecies is the reactant (i.e. non-zero initial concentration), and all the other pseudospecies are the products. The infinite sink approximation is applied to the products, namely their concentration can only increase in time, similarly to some approaches used to determine phenomenological rate constants from ME simulations [14]. This results in the exponential decay of the reactant. The concentration profiles of the lumped system $\frac{d\tilde{\mathbf{c}}}{dt} = \tilde{\mathbf{K}}\tilde{\mathbf{c}}$ are then derived from those of the detailed system. Thanks to the exponential decay of the reactant, lumped rate constants constituting matrix $\tilde{\mathbf{K}}$ are approximated from a simple differential fit of the product concentration profiles formed from each pseudospecies. The lumped mechanism thus derived is validated with simple 0D isothermal and isobaric simulations comparing the concentration profiles obtained from the detailed and lumped kinetic mechanisms.

The derivation of lumped rate constants of a pseudospecies constituted of merged species (e.g. $C_5H_{10}OOH$-1 consists of four isomers of the detailed scheme) requires setting an initial composition for the simulations of the detailed scheme $\frac{d\mathbf{c}}{dt} = \mathbf{Kc}$. In the case of the RO_2 PESs the composition of each lumped QOOH was derived at each temperature with 0D simulations of the detailed mechanism of RO_2 PES. For instance, Figure 2 shows the branching fractions of the four species constituting $C_5H_{10}OOH$-1 (see Figure 1) as a function of temperature. The profiles were obtained from isothermal simulations of the reactivity of RO_2 PES accessed from C_5H_{11}-1+O_2. A correct composition of POOH isomers is essential to reproduce the low temperature chemistry of n-pentane. For instance, choosing the equilibrium composition within each isomer pool (e.g. derived from the thermochemistry) completely fails to reproduce the negative-temperature-coefficient (NTC) behavior in the ignition of n-pentane.

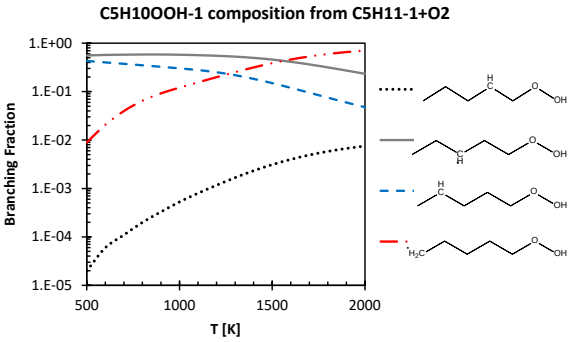

Figure 2: Composition of $C_5H_{10}OOH$-1 lumped species derived from the reactivity of C_5H_{11}-1+O_2.

The composition of the products of O_2 addition to n-pentyl was then used for the derivation of the secondary reactivity of the merged pseudospecies $C_5H_{10}OOH$-1,2,3 and $C_5H_{10}O$, as sketched in Figure 3. For example, the composition of $C_5H_{10}OOH$-1 of Figure 2 was also set as the initial composition for the simulations of the detailed mechanism of O_2 addition to $C_5H_{10}OOH$-1, namely for the lumping of RO_4 PES.

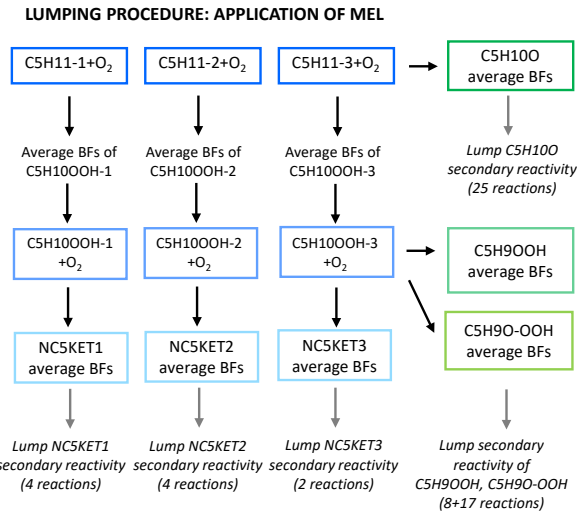

Figure 3: Schematic procedure of the application of MEL to R+O_2 and QOOH+O_2 PESs and the secondary reactivity of the products.

RO_4 PES is accessed from O_2 addition to POOH isomers. Since the lumping of RO_2 and RO_4 PESs must be done consistently, the POOH pseudospecies constituents (see Figure 1) and their composition was set identical to RO_2 PES. As opposed to RO_2 PES, in this case the pool of $P(OOH)_2$ isomers does not interact with any of the other species in the mechanism. Similarly to the hydroperoxyl-alkyl radicals of RO_2 PES, their reactivity is extremely fast, such that $P(OOH)_2$ isomers do not show significant accumulation in the system. For instance in the simulations automatically performed with MEL the mole fraction of any of the $P(OOH)_2$ isomers was always below 10^{-4}. For this reason, none of the $P(OOH)_2$ species was included among the pseudospecies of the lumped mechanism, thus reducing the number of species by 16. The lumping procedure adopted was the same as that described above. In this case, both the olefins and the cyclic ethers product sets were lumped together as two merged pseudospecies. On the other hand, the carbonyl-hydroperoxides were lumped as three different pseudospecies; each group derives from the non-interconnected lumped hydroperoxyl-alkyl radicals $C_5H_{10}OOH$-1,2,3. Figure 4 shows an example of MEL simulations of the validation of the reactivity of RO_4 PES accessed from $C_5H_{10}OOH$-1+O_2. Both the decay of the $C_5H_{10}OOH$-1 radical and the accumulation and consumption of the hydroperoxyl-alkyl-peroxyl radical are extremely well reproduced by the lumped model, as well as the formation of products, with slight discrepancies at higher temperatures.

Overall, the lumping of RO_2 and RO_4 PESs led to the significant reduction of a detailed mechanism of 81 species and 151 reaction to a lumped mechanism of 20 species and 56 reactions. The most significant reduction results from the lumping of RO_4 PES, as highlighted also in Figure 1. MEL also allows further optimization of the rate constants derived using profiles such as those of Figure 4 using OptiSMOKE++ [15]. However, in this case we did not perform this additional step both thanks to the good results obtained and because of illustrative purposes.

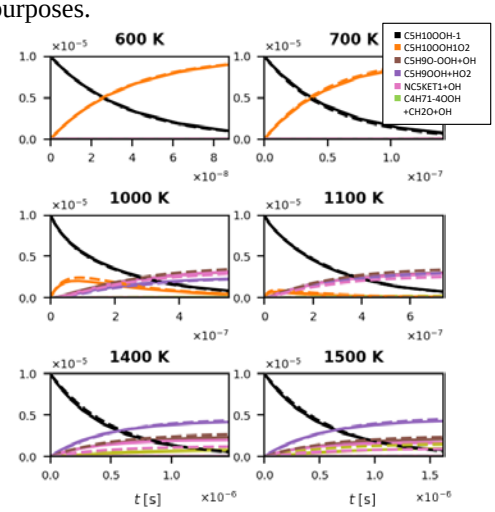

Figure 4: Example of MEL simulations for the validation of the lumping of C5H10OOH-1 reactivity. Solid and dashed lines are the results of the detailed and lumped submechanisms of RO_4 PES, respectively.

Lumping of the secondary reactivity of products

The lumped cyclic ethers derived from QOOH and all the products of the second O_2 addition to QOOH isomers further decompose to smaller species. Their detailed reactivity was therefore lumped according to the temperature-dependent composition of each merged pseudospecies obtained from the lumping of RO_2 and RO_4 PESs. In this case, the level of detail of the decomposition of the products was fully retained, mostly because their reactivity is part of different portions of the mechanism, and a lumping of the full mechanism is out of the scope of this work. Therefore, there was no significant reduction in the number of secondary reactions (61 reactions resulted in 51 lumped reactions).

Each of the $C_5H_{10}OOH$-1,2,3 pseudospecies produces $C_5H_{10}O$ with a given composition; in addition, not all $C_5H_{10}O$ isomers are produced by each QOOH radical. Therefore, the final composition of $C_5H_{10}O$ is determined both by the branching fractions of its constituents produced by each QOOH pseudospecies and by the total production rate of $C_5H_{10}O$ from the QOOH selected. Considering, for example, the decomposition of one of the cyclic ethers in the detailed mechanism $C_5H_{10}O1$-2+HO_2 => C_2H_3CHO+C_2H_5+H_2O_2 with rate constant $k_{i\rightarrow P}$: this reaction was lumped to $C_5H_{10}O$+HO_2 => C_2H_3CHO+C_2H_5+H_2O_2 rescaling its reaction rate as

$$k(T)_{i\rightarrow P} \cdot \sum_{QOOH} BF(T)_{i,QOOH} \cdot \frac{k(T)_{QOOH\rightarrow C_5H_{10}O}}{\sum_{QOOH} k(T)_{QOOH\rightarrow C5H10O}}$$

where the sum runs over the three hyroperoxyl-alkyl radicals, $BF_{i,QOOH}$ are the branching fractions of ether i ($C_5H_{10}O1$-2 in this example) produced by each QOOH and $k_{QOOH\rightarrow C_5H_{10}O}$ is the lumped rate constant for the total production of $C_5H_{10}O$ by each QOOH. All quantities were fitted according to modified Arrhenius expressions so as to retain accurate temperature dependence easily integrated in the final kinetic model. A simple averaging of the rate constants of the decomposition reactions of cyclic ethers instead fails to reproduce the NTC behavior of n-pentane and causes an underestimation of the reactivity in simulations of ideal reactors experiments.

The lumping of the secondary reactivity of olefins and cyclic ethers produced from the second O_2 addition to QOOH radicals was done using the approach described above. The lumping of the secondary reactivity of carbonyl-hydroperoxides was instead simpler. In fact, we considered three different isomers NC_5KET1,2,3 each produced by a different QOOH pseudospecies, as shown in Figure 1. Therefore, the scaling of the corresponding rate constants only required to consider the composition of each lumped carbonyl-hydroperoxide. For instance, the rate constants of the decomposition reactions of NC_5KET1 produced from $C_5H_{10}OOH$-1 were derived from those of the detailed mechanism as $k(T)_{i\rightarrow P} \cdot BF_{i,C_5H_{10}OOH-1}$, where i is one of the four constituents of NC_5KET1 and $BF_{i,C_5H_{10}OOH-1}$ is the branching fraction of isomer i as derived from the reactivity on RO_4 PES accessed from $C_5H_{10}OOH$-1+O_2.

Results of kinetic simulations

The validation of the lumping approach proposed was finally performed with kinetic simulations of ideal reactor experimental data of n-pentane oxidation. All kinetic simulations were performed with OpenSMOKE++ [16]. In particular, we simulated jet stirred reactor (JSR) experiments [13], shock tube (ST) experiments [12] and rapid compression machine (RCM) experiments [9] in the 1-25 atm pressure range at different equivalence ratios (ϕ = 0.3-2). The data were simulated with both the detailed n-pentane oxidation model of Bugler et al. [12] and with the lumped model derived in this work, i.e. model in [12] with the low-temperature n-pentane subset replaced by the lumped one. The thermochemistry of the merged pseudospecies of the lumped model corresponds to that of the most abundant isomer in each pseudospecies, as it is often done in traditional chemical lumping approaches [17].

The results of the kinetic simulations are shown in Figure 5. It is evident that the lumped model reproduces the results of the detailed model accurately. In particular, in the case of JSR experiments (Figure 5c) the two lines are almost superimposed. Only minor discrepancies in smaller products such as CH_3CHO and CH_2O are found. A similar agreement is found for the ignition delay times (IDTs) measured in ST experiments (Figure 5a): above 1000 K, there is no difference between the detailed and lumped models. This is expected, as the lumping of low-temperature oxidation pathways does not impact the high-temperature ignition behavior. Below 1000 K instead, the reactivity of the lumped model is slightly underestimated. Hence, the simulated IDT overpredicts that of the detailed scheme by a maximum of 17% at 900 K and ϕ = 1, 2. The highest discrepancies are found in the IDTs measured in RCM experiments in the 600-1100 K temperature range (Figure 5b). In this case, the lumped model overpredicts the IDTs by about 20-30% with respect to the detailed model at about 800-900 K. In particular, the maximum difference between the two models is about 35% at 820 K and 10 atm at both ϕ = 1, 2. Despite this, the overall trends of the NTC behavior are very well reproduced by the lumped model, considering that no optimization of the lumped rate constants was performed and that no kinetic simulations of ideal reactors data were performed for model validation prior to those presented in this section.

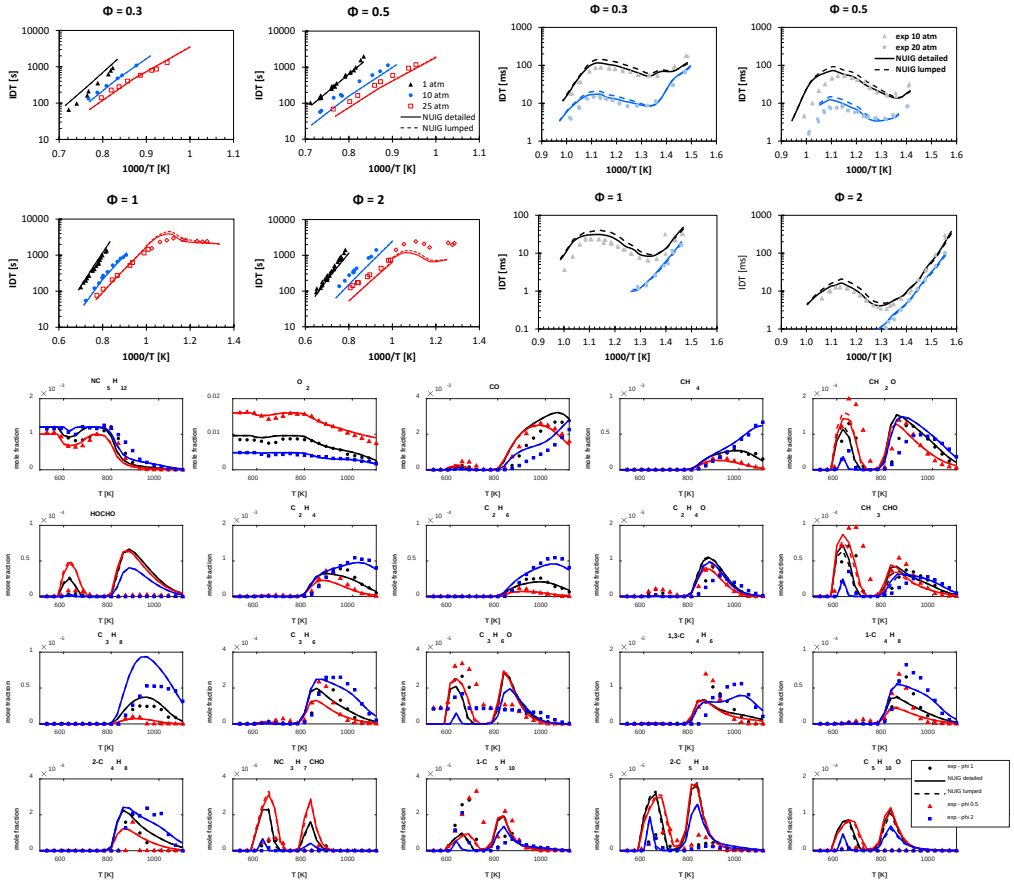

Figure 5: Simulation results versus experimental data of a) shock tube experiments at P = 1, 10, 25 atm and Φ=0.3, 0.5, 1, 2, b) rapid compression machine experiments at P = 10, 20 atm and Φ=0.3, 0.5, 1, 2, c) jet stirred reactor experiments at 10 atm and Φ=0.5, 1, 2 [9,12,13]. In a), c), simulation results with the detailed and lumped mechanisms are represented by solid and dashed lines, respectively. In b), stars * for the detailed model and diamonds ◊ for the lumped model are used.

Conclusions

In this work, we presented the application of an automatic chemical lumping approach recently developed at CRECK to the low-temperature oxidation chemistry of n-pentane [4]. Among other reasons, the need of developing automatic lumping procedures able to retain the chemical significance of detailed mechanisms stems from the increasing number of theoretical

calculations and complexity of chemical pathways performed for the update of kinetic mechanisms with more accurate rate constants. The inclusion of the results of theoretical calculations for complex multi-well PESs into kinetic schemes is still a challenging theoretical task and often results in introducing into the final kinetic scheme a large number of additional species, most of which generally do not accumulate significantly in macroscopic kinetic simulations nor show any secondary reactivity. Our lumping methodology (MEL) automatically implemented with a python code processes the output of ME calculations for multi-well PESs or any detailed mechanism describing the reactivity of multiple interconnected isomers on one PES. MEL is able to derive a smaller set of pseudospecies and equivalent rate constants able to reproduce the macroscopic chemical behavior of the detailed mechanism without the need of any experimental data or simulations of several types of ideal reactors at different conditions. The reactivity of redundant species is implicitly included in the kinetic mechanism, whereas species with similar chemical behavior are merged as one pseudospecies. MEL also provides the temperature and pressure dependent composition of each pseudospecies, such that the inclusion of the detailed secondary reactions and a detailed product distribution from each isomer is still possible. In this paper, we applied MEL to the low-temperature oxidation chemistry of the detailed n-pentane combustion model of Bugler et al. [12], recently revised in light of new theoretical findings. In particular, we lumped the RO_2 and RO_4 PESs and adapted the secondary reactivity of lumped products to the merged pseudospecies introduced. The lumping consisted of three steps: first, we lumped RO_2 PES. We chose to retain most of the level of detail of the original mechanism, lumping only the hydroperoxyl-alkyl radicals as three merged pseudospecies and all cyclic ethers as one single pseudospecies. Then, we lumped RO_4 PES consistently with the hydroperoxyl-alkyl radicals distribution derived from the lumping of RO_2 PES. In this case, we were able to implicitly include into the lumped mechanism the full reactivity of the dihydroperoxyl-alkyl radicals (i.e. no dihydroperoxyl-alkyl radical species was explicitly introduced), and we merged as single pseudospecies both the olefins and the cyclic ethers. The carbonyl-hydroperoxides were instead merged as three different pseudospecies. Overall, our lumping reduced a detailed sub-mechanism of 81 species and 151 reactions to only 20 species and 56 reactions. Finally, we lumped the secondary reactivity of products according to the merged product pseudospecies composition derived in the previous steps. The lumped model thus obtained was validated against the detailed model simulating ideal reactor experimental data of shock tube, rapid compression machine, and jet stirred reactor experiments, obtaining an excellent agreement between the two models. These results support the accuracy of the approach proposed and encourage its application to both existing detailed mechanism and to the exploration of new and complex PESs when the aim is to include the findings in predictive kinetic models. MEL could be also useful in hierarchical automated model generation tools as those currently being developed in the context of DOE ECP project [18].

References

[1] P. Pepiot, L. Cai, H. Pitsch, in: Math. Model. Gas-Phase Complex React. Syst. Pyrolysis Combust., 2019, pp. 799–827.

[2] M.I. Strelkova, A.A. Safonov, L.P. Sukhanov, S.Y. Umanskiy, I.A. Kirillov, B. V. Potapkin, H.J. Pasman, A.M. Tentner, Combust. Flame 157 (2010) 641–652.

[3] G.R. Galimova, V.N. Azyazov, A.M. Mebel, Combust. Flame 187 (2018) 147–164.

[4] L. Pratali Maffei, M. Pelucchi, C. Cavallotti, A. Bertolino, T. Faravelli, Chem. Eng. J. (2021) under review.

[5] E. Ranzi, M. Dente, A. Goldaniga, G. Bozzano, T. Faravelli, Prog. Energy Combust. Sci. 27 (2001) 99–139.

[6] L. Pratali Maffei, M. Pelucchi, T. Faravelli, C. Cavallotti, React. Chem. Eng. 5 (2020) 452–472.

[7] L. Pratali Maffei, T. Faravelli, C. Cavallotti, M. Pelucchi, Phys. Chem. Chem. Phys 22 (2020) 20368–20387.

[8] L. Cai, H. Pitsch, S.Y. Mohamed, V. Raman, J. Bugler, H. Curran, S.M. Sarathy, Combust. Flame 173 (2016) 468–482.

[9] J. Bugler, K.P. Somers, E.J. Silke, H.J. Curran, J. Phys. Chem. A 119 (2015) 7510–7527.

[10] K. Zhang, C. Banyon, C. Togbé, P. Dagaut, J. Bugler, H.J. Curran, Combust. Flame 162 (2015) 4194–4207.

[11] E. Ranzi, C. Cavallotti, A. Cuoci, A. Frassoldati, M. Pelucchi, T. Faravelli, Combust. Flame 162 (2015) 1679–1691.

[12] J. Bugler, B. Marks, O. Mathieu, R. Archuleta, A. Camou, C. Grégoire, K.A. Heufer, E.L. Petersen, H.J. Curran, Combust. Flame 163 (2016) 138–156.

[13] J. Bugler, A. Rodriguez, O. Herbinet, F. Battin-Leclerc, C. Togbé, G. Dayma, P. Dagaut, H.J. Curran, Proc. Combust. Inst. 36 (2017) 441–448.

[14] A. Barbato, C. Seghi, C. Cavallotti, J. Chem. Phys. 130 (2009) 074108.

[15] M.B. Fürst, A. Bertolino, A. Cuoci, T. Faravelli, A. Frassoldati, A. Parente, Comput. Phys. Commun. under Rev. (2021).

[16] A. Cuoci, A. Frassoldati, T. Faravelli, E. Ranzi, Comput. Phys. Commun. 192 (2015) 237–264.

[17] S.S. Ahmed, F. Mauß, G. Moreácz, T. Zeuch, Phys. Chem. Chem. Phys. 9 (2006) 1107–1126.

[18] D.P. Zaleski, R. Sivaramakrishnan, H.R. Weller, N.A. Seifert, D.H. Bross, B. Ruscic, K.B. Moore, S.N. Elliott, A. V. Copan, L.B. Harding, S.J. Klippenstein, R.W. Field, K. Prozument, J. Am. Chem. Soc. (2021) jacs.0c11677.